APRIL
2005

fea INFORMATION

WWW.FEAINFORMATION.COM

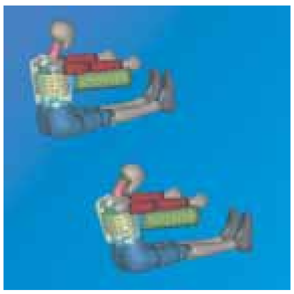

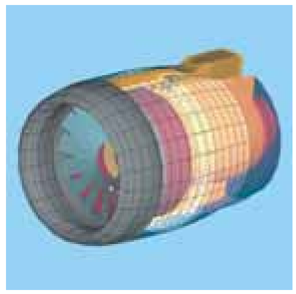

COVER STORY

INTEL

VISUALIZATION: BRINGING FLEXIBILITY AND NEW CAPABILITIES TO COMPUTING PLATFORMS

TECHNICAL SPOTLIGHT

CRAY

LS-DYNA CERTIFIED FOR CRAY XD1 SUPERCOMPUTER

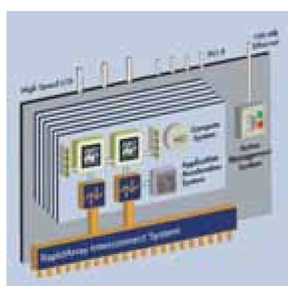

TECHNICAL SPOTLIGHT

FUJITSU

PRIMEQUEST: RELIABILITY AND SECURITY IN OPEN SYSTEMS

FEA INFORMATION RESOURCE MAGAZINE

FEA Information Worldwide Participant's

Contents

02	FEA Information Inc. Announcements
03	Cover Story INTEL
07	Technical Spotlight CRAY
10	Technical Spotlight FUJITSU
14	Industry News
15	Asia Pacific News
16	Available Paper: Transient Response of a Projectile in Gun Launch Simulation Using Lagrangian and ALE Methods
17	Resume: Philip Burnside
21	Events
22	LS-DYNA Resource Page
26	Directory – Hardware & Computing and Communication Products
27	Directory - Software Distributors
29	Directory – Consulting and Engineering Services
30	Directory – Educational & Contributing Participants
31	Directory – FEA Informational Websites
32	Directory – Archived Site News
33	Top Crunch News

FEATURED PUBLICATION: Published by Dr. David Benson

Editor: Trent Eggleston **Managing Editor:** Marsha Victory **Technical Editor:** Art Shapiro **Graphic Designer:** Wayne L. Mindle	**Technical Writers:** Dr. David Benson Uli Franz Dr. Ala Tabiei **Technical Consultants:** Steve Pilz Reza Sadeghi

FEA Information Announcements

Our first international ad

Please see our ad under Asia Pacific News
Ad created by our Graphics Editor, Dr. Wayne Mindle.

New Menu Bar Link:
www.feainformation.com Link "Hardware"

Travel:

Marsha Victory will be attending the 5th European LS-DYNA Conference UK 05/25-26/05 (Arup). Our technical editor, Arthur Shapiro will be attending and presenting a paper. If you are attending please say hello.

Additionally, Arthur Shapiro, just returned from CADFEM, Stuttgart, Germany where he presented the course, Using LS-DYNA for Heat Transfer & Thermal-Stress Problems on April 21-22. The course objective was to provide an understanding of computational finite element heat transfer. Topics included how to select an appropriate time step, thermal boundary conditions, techniques in solving non-linear problems, thermal contact, and special topics (e.g., modeling honeycombs, powders, MEMS). This was followed by methods to solve coupled thermal-stress and thermal-fluid problems.

Training:

LSTC Michigan is pleased to announce the first two training courses available at their Michigan location:

Implicit LS-DYNA, May 25-27
Introduction to LS-DYNA, June 8-10
Contact classes@lstc.com for information

Sincerely,
Trent Eggleston & Marsha Victory

Cover Story: Virtualization: Bringing Flexibility and New Capabilities to Computing Platforms

Francis J. Bruening Senior Marketing Manager Corporate Technology Group Intel Corporation

R.M. Ramanathan Senior Software Architect Corporate Technology Group Intel Corporation

Overview: Making PCs Easier to Use

The perceived complexities of computing systems are a deterrent to their pervasive adoption by users. The convergence of computing and communications can drive continuing growth, but this growth will not be sustainable unless we can find new ways to transparently manage complexities and hide them from users.

This article and the paper from which it is derived provide a conceptual overview of a new concept – platform virtualization – that can be used to provide end-users with future computing systems that are as easy to use as consumer electronics equipment. Virtual platforms promise to make future computers more autonomous, reliable and trusted, making them an almost invisible tool in our day-to-day lives. Platform virtualization is a key enabler of new usage models designed to make these goals a reality. It is the road to the future of computing.

The Path to the Future

The doubling of transistor density on integrated circuits approximately every two years, known as Moore's Law, has enabled the computer industry to build increasingly powerful and complex systems that deliver dramatic and sustained improvements in price/performance. The result is that PCs, mobile computers, and converged computing and communications devices such as cell phones and PDAs have become progressively more feature-rich and powerful.

Despite these gains, sophisticated computing devices and applications are seen as complex and intimidating by many users. Such complexities can include the effort required to learn new applications, the perceived difficulty of transferring files and data from legacy systems to replacement platforms, the challenge of software updates, and concerns over security. Unless it can be remedied, the issue of complexity looms as a barrier to future industry growth.

Today the challenge for the industry is to continue building smaller, thinner and faster computing systems, while finding better ways to manage the complexities of computing technologies. The industry is focusing a great deal of effort on securing and managing information and devices, on making computing more flexible and ubiquitous, and on building resilience into computing systems to make them available to users anytime and anywhere. The concept of platform virtualization provides the path to the future of powerful, autonomous, reliable and trusted computing devices.

Platform virtualization can be defined as the creation of a logically partitioned computing system that runs on top of an actual platform. While virtualization has been applied to storage and servers, the concept of platform virtualization goes further to include all layers of the platform – from applications and operating software to platform components, processors and interconnects.

Virtual platforms are perceived by users –and function in all respects – as if they were physical computers. Because they are abstracted and partitioned from underlying platforms and from each other, virtual platforms provide an easily transportable, extremely robust technique for hiding complexity from users while enhancing system security.

Virtualization provides a way to create less-complex systems that partition the subsets of computing systems into more manageable instantiations. In addition, partitioning can provide more security to systems, networks and applications by isolating potentially vulnerable subsystems from underlying system resources and from other virtual platforms.

Ending the PC Update Blues

Desktop computers are becoming much more affordable. For under $1,000 a consumer can buy a powerful computer complete with software applications, productivity tools and connectivity software. Increasing numbers of users now view the PC as an entertainment appliance that enables them to play games, communicate via e-mail, and shop on the Internet. Even with the popularity of PCs, the thought of updating or maintaining their systems can be intimidating to many consumers.

Platform virtualization can make the PC upgrade and maintenance process invisible to users. Consider Joe, who has been using his old computer system for five years. He uses it to store confidential data, contact information, personal financial and family information, tons of old e-mails, browser favorites, and his kids' games.

Joe is very comfortable with his old computer and its user interface and does not want to risk losing his personal information and organizational structure. As much as he might want the performance of a new PC, he is nervous about upgrading because he has heard horror stories from friends who have lost data or file structures after upgrading to a new PC or operating system. Joe is also nervous about performing what he perceives to be complex maintenance and security enhancements.

Platform virtualization can relieve Joe's anxiety about PC upgrades by emulating his old computer on the new system and by meeting these essential criteria:

1. When upgrading, Joe must be able to migrate from old to new computer or operating system with a simple installation process. After the migration is complete, the new system must be familiar and stable.
2. Any upgrades will bring increased benefits, including performance, functionality, and security, but the new system must maintain familiar user interfaces to minimize learning curves.
3. The old system should be accessible in the new computer with a simple user interface such as a desktop icon.
4. All peripherals, including the printer, must work and behave exactly the same way they did before. This applies whether Joe is installing a new operating system, application or security updates.

5. Moving data and the familiar desktop environment from the old computer to the new system should be as easy as a mouse click. The new computing environment must provide management controls that enable Joe to migrate the system however and whenever he wants.
6. The emulated old computer must be secured with appropriate access controls and confidentiality in the new computing environment.
7. The emulated old computer must not introduce any security risks or performance problems to the new computer and applications.

By compartmentalizing system complexities, platform virtualization enables Joe to easily migrate and maintain his familiar computing environment, while making his system more manageable.

"Any Computer Is My Computer"

Future technology advancements may create virtualization environments where any computer could be used by any user at any time while keeping the interface the same. Consider this possible future scenario:

Our friend Joe is working on a presentation at home on his personal computer. On his home system he uses the same environment he does at work, including the same operating system, software applications, and IT policies. His home and office systems are virtually identical.

Now, Joe needs to fly to a business conference. In the airport, a virtual environment that mirrors his home and office environment appears on a public computer. Whether Joe is at home, at work or on the road using a public computer, virtualization ensures that his computer environments are virtually identical.

To access the virtual computing environment, Joe might log-in using his thumbprint or a smart card or some other type of biometric authentication. This technology enables Joe to access his virtual computer using any physical hardware anywhere in the world. Although Joe does not necessarily own the physical computer he is working on at any given time, he does own the computing environment. The physical hardware can be anything from a PC to a PDA or even an advanced cell phone.

Virtualization uses overlays of the network using the power of the local computer. The user can always keep the personal environment, the *virtual computer*, in a keychain dongle and insert it into the public computer to begin working. In this way, platform virtualization creates a transparent, personalized computer environment.

Working in conjunction with academic research and industry participants, Intel Research is conducting two projects, PlanetLab and Internet Suspend/Resume (ISR). The goal of these projects is to apply virtualization technologies to create transparent and personalized user experiences while providing unprecedented scalability for secure, autonomous, and flexible systems.

Foundation for the Future

Virtualization lays the foundation for future computing systems and platform design. As shown in **Figure 1**, virtualization is rooted in every layer of the computing system, from applications to platform components, interconnects, and processors. Supporting virtualization in every layer of the hardware ensures that computing systems are secure and autonomous and that complexities are managed transparently.

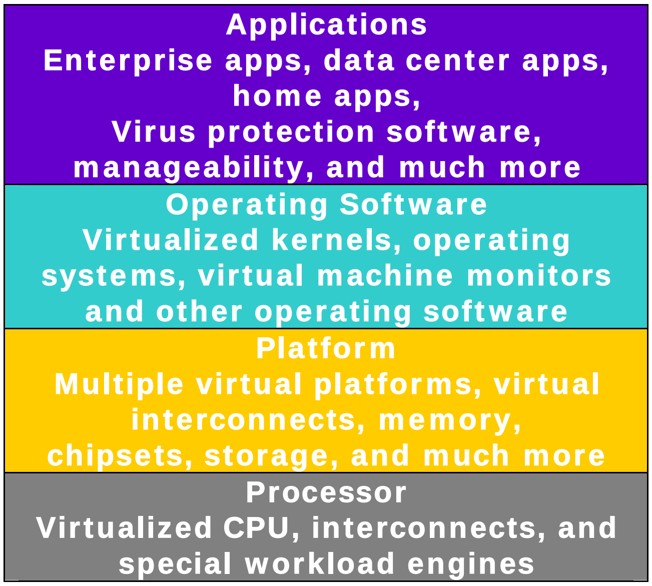

Figure 1. Virtualization is rooted in every layer of the computing platform.

In the future, a single physical computer will support sets of multiple virtual computers or virtual partitions, some of which will be dedicated to the operating system and special-purpose applications, with others reserved for general purpose computing tasks. Virtualization provides endless possibilities for the design of future computers.

Summary:

Computing and connectivity are increasingly inseparable. Virtualization will ensure that the connected network of the future is trusted, secured and autonomous. Users will not need to worry that a partitioned virtual system that contains valuable files will be attacked by viruses or malicious hackers, and users will never need to worry about updating software patches to keep their systems secure.

Virtualization also enables limitless possibilities in platform and applications design, while making manageability and security transparent to users.

For more information go to www.intel.com

PRODUCT SPOTLIGHT: Cray XD1 Supercomputer

LS-DYNA Certified for Cray XD1 Supercomputer

A new player in the Linux / Opteron system arena, the Cray XD1™ supercomputer is coming on strong in the real application performance race. Recently certified by Livermore Software Technology Corp. (LSTC) for LS-DYNA software, the Cray XD1 system posted top scores on LS-DYNA benchmark tests on www.topcrunch.org.

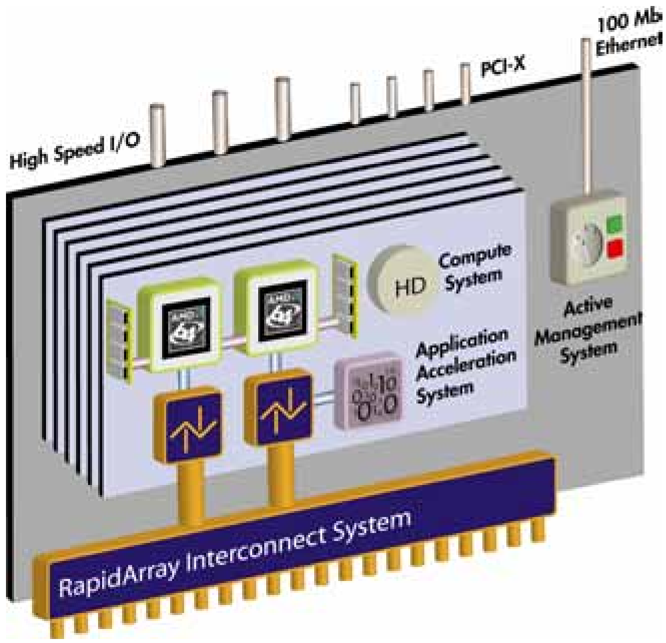

Linux, Opteron computing for CAE applications, Linux x86 based, 32 and 64-bit compatible, with support for common programming paradigms like MPI and shared memory access models like Shmem and Global Arrays, the Cray XD1 supports a wide variety of CAE applications.

CAE applications need more than high performing processors. They require superior memory, interconnect and I/O performance to match the processor performance. Exceptional application efficiency can only be achieved in a balanced system that matches processing power with memory, interprocessor bandwidth and I/O bandwidth. By providing all of these the Cray XD1 system offers a powerful alternative to the cluster solutions choices.

Three-Car Collision Test

In the LS-DYNA three-car collision benchmark test, the Cray XD1 supercomputer performed from 9 to 29 percent faster than competing 32 processor systems. Using 64 processors, the Cray XD1 system outpaced other clusters by as much 12 percent, indicating its superior scalability. Similar leading results were demonstrated on the LS-DYNA neon-refined benchmark.

“The performance advances demonstrated by the Cray XD1 system make our code even more valuable to the engineers who use it to simulate collisions, structural failures, explosions, earthquakes, and other difficult-to-model problems that have important real-world consequences," said Dr. John Hallquist, president, LSTC. "The Cray XD1 supercomputer and the LS-DYNA application offer the CAE community a solution that provides optimal performance, functionality, and scalability."

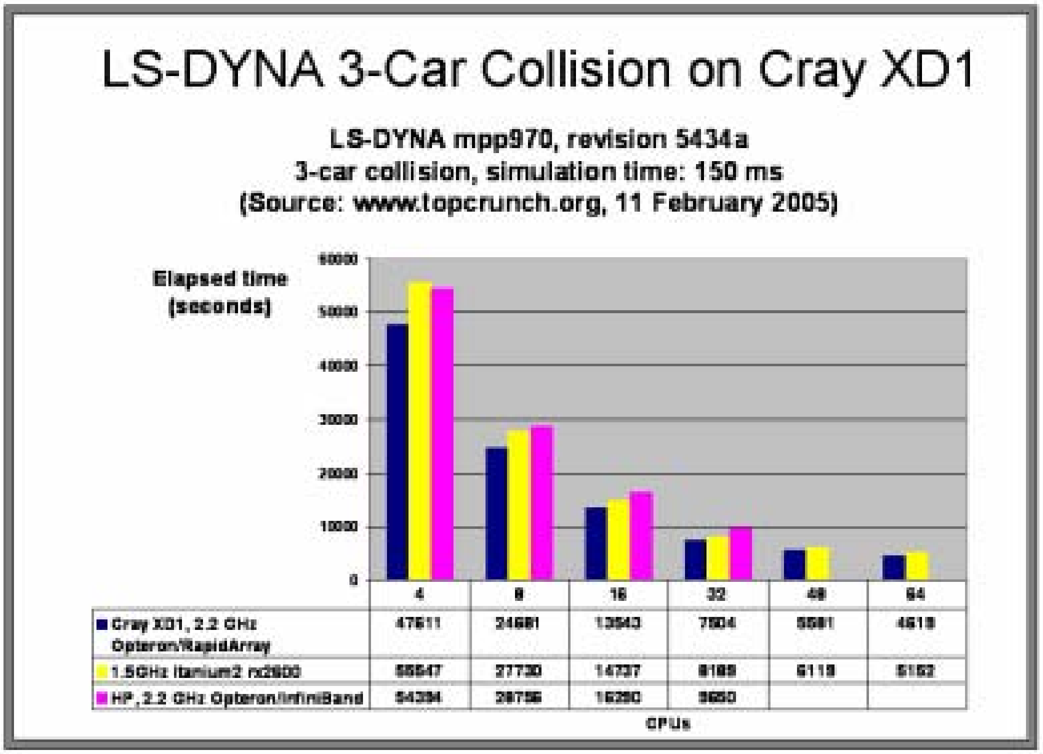

The pressure to meet ever-shrinking product design cycle timelines drives CAE end-users to deploy jobs using higher processor counts. While the parallel implementation of CAE software has improved dramatically, the limitations in hardware technology used in commodity systems has not been able to fully exploit the true potential of software. Consequently, the system efficiency may rapidly start deteriorating at higher processor counts, and make it difficult for the CAE user to justify system utilization in that processor range.

The Cray XD1 supercomputer offers the CAE community the ability to perform high fidelity simulation as they strive to push the limits of application scalability.

The RapidArray interconnect is the key to the scalability performance of LS-DYNA on the Cray XD1 supercomputer. The Cray XD1's AMD Opteron™ processors are connected directly to a high performance interconnect—the RapidArray interconnect—eliminating both the shared resource contention, seen in SMP servers, and the PCI bus bottlenecks, seen in commodity clusters. This interconnect provides up to 30 times higher bandwidth and a 1.7 microsecond MPI latency, 70 times lower latency than common cluster interconnects.

In addition, the RapidArray switching fabric provides several fold better bandwidth than any other interconnect in the market today. With interconnect bandwidth on par with memory bandwidth, a major system bottleneck is removed for many applications, improving performance and simplifying software development. The dramatic improvement in bandwidth and latency leads directly to better application scalability.

"The LS-DYNA benchmarks spotlight how the Cray XD1 system's superior interconnect technology and synchronized scheduling capabilities deliver faster times to solution than other high-performance computing (HPC) systems—at prices starting under US$100,000," said Himanshu Misra, Cray CAE business manager. "Furthermore, the Cray XD1 system sustains this exemplary efficiency when scaled to higher processor counts, allowing LS-DYNA users to increase overall throughput and run larger, more complex simulations."

The Cray XD1 supercomputer also offers CAE users the Active Manager subsystem, which simplifies system administration and management, and lets users focus on their CAE application. Both these features translate into higher throughput and greater return on CAE investment.

BENCHMARK DETAILS

1. Computer System: CRAY XD1
    a. Vendor: CRAY
    b. CPU Inerconnects: Rapid Array
    c. MPI Library: CRAY XD1 MPI
    d. Processor: AMD Opteron 2.2 GHZ
    e. Number of nodes: 32
    f. Processors/Nodes: 2
    g. #Nodes x #Processors per Node = 64 (*Total CPU*)
    h. Operating System: Suse Linux 8
2. Code Version: LS-DYNA
3. Code Version Number: mpp970, 5434a
4. Benchmark problem: neon_refined
5. Wall clock time: 380
6. RAM per CPU: 2
7. RAM Bus Speed: *Information Not Provided*
8. Benchmark Run in Single or Double precision: Single
9. Benchmark Run SMP or MPP: MPP
10. System Dedicated/Shared: Shared
11. Location: Chippewa Falls
12. Submitted by: Ting-Ting Zhu
13. Submitter Organization: CRAY Inc.

Product Data Sheet:

CRAY XD1

The Cray XD1TM supercomputer combines breakthrough interconnect, management and reconfigurable computing technologies to meet users' demands for exceptional performance, reliability and usability.
www.cray.com/downloads/Cray_XD1_Datasheet.pdf - 876KB - 02 Oct 2004

For more information go to www.cray.com

PRODUCT SPOTLIGHT: FUJITSU

PRIMEQUEST: Reliability and Security in Open Systems

www.fujitsu.com/global/services/computing/server/primequest/documents/featurestory.htm

By introducing PRIMEQUEST, Fujitsu is extending the boundaries of reliability computing. They are removing barriers to the use of commodity products for the most important and demanding business and IT infrastructure tasks. The cost benefits of open systems have long been known, but until now, many organizations seeking mission-critical operation have had to forego those benefits because of reliability and scalability concerns. Instead they have limited their choice to the high reliability and business continuity benefits available with more proprietary systems.

PRIMEQUEST supports the growing capabilities of Windows and Linux systems into the mission critical arena by providing hardware platforms designed using mainframe-derived levels of hardware reliability, availability and serviceability (RAS). This leaves Windows and Linux customers free to enjoy investment protection, freedom of choice and unlimited growth when provisioning for future growth, without compromise.

Further, PRIMEQUEST meets the needs of Open Systems organizations looking to maximise their existing Linux and/or Windows skills with top-to-bottom coverage in the data center. No longer will growing organisations have to learn a new skill-set just to implement the highest levels of business support.

Designed using principles, engineering technology and Fujitsu know-how garnered from decades of high reliability development, PRIMEQUEST conforms to Fujitsu's TRIOLE Open Systems' business continuity, business agility, and business efficiency standards for open systems. PRIMEQUEST like all of Fujitsu's mission critical systems also matches
the expectations of customers looking at the next generation of "autonomous" computing

Business continuity comes from architecture with fault immunity included at every level. The Intel® Itanium® 2 processors and Fujitsu chipset in combination, deliver the best industry standard implementation of RAS. At the systems level there is unmatched error prevention and redundancy. The new "System Mirror" means memory modules and crossbar interconnects all operate in duplex mode. Errors can be isolated without system halt, for exemplary systems' operation continuity. Flexible I/O (FIO) means I/O resources can match real-time performance requirements on-demand. Such flexibility and standard redundancy means even maintenance downtime can be reduced by up to 90% compared with current industry figures.

To further strengthen Linux for business critical use, about 500 Fujitsu developers are contributing to the open-source community. This and the joint development organisation with Red Hat, as embodied in Red Hat Enterprise Linux AS (v.4 for Itanium) used with PRIMEQUEST.

Fujitsu is also working closely with Microsoft, under the Global Alliance Partnership, to deliver fail-safe environments for mission-critical operation of Windows applications.

For business efficiency and flexibility new technologies allow up to 8 partitions to operate safe from any single point of failure. Each fully independent PRIMEQUEST partition provides the flexibility and operational characteristics of the system as a whole. Running in parallel partitions, Windows and LINUX resources, including memory, CPU and I/O can be independently and dynamically adjusted to match load requirements throughout the day. This means PRIMEQUEST is quick to adapt to change whilst always delivering excellent resource efficiency, flexibility and stability.

Customer choice is also a winner, with PRIMEQUEST fully rounding out Fujitsu's server infrastructure offerings. Whatever the requirement and whatever the application environment, Fujitsu now offers the right mission critical platform solution across the broadest range of solutions. PRIMEQUEST fully compliments Fujitsu's ongoing mainframe and UNIX PRIMEPOWER products, making Fujitsu the expert place to go for business critical computing of all flavours.

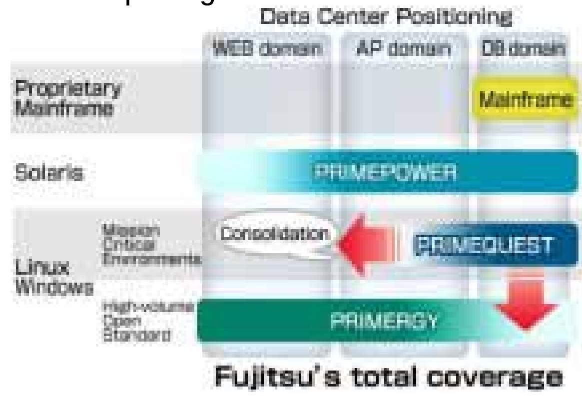

PRIMEQUEST's elegant design underpins its sophistication. At its heart is the powerful Intel® Itanium® 2 processor with its EPIC architecture. But it is the way this power is used and controlled that sets PRIMEQUEST apart.

Scalable to 32 (64 with new generation dual core CPUs) processors in a single cabinet, it can be configured as 1 to 8 flexible fully independent partitions. Able to host Windows and/or Linux, 32-bit or 64-bit applications, in any combination, it is ideal for server consolidation. Administration is simplified by in-built redundant ManageMent Boards(MMB). These not only control resource allocation but also automate administration and recover potential system faults.

PRIMEQUEST's mission critical profile comes from full component redundancy and System Mirror, where even part system boards are electrically isolated. Add in its separation of I/O from CPU and Memory, redundant high-speed cross bars and Fujitsu's PRIMECLUSTER environment, and it delivers the industry's fastest recovery times and up to 99.999% availability.

Typical of the attention to detail is the revolutionary cable management. Normally large servers require tens if not hundreds of cable connections. This management overhead is removed in

PRIMEQUEST, as all cabling is integrated into the backplane. No physical cable adjustments are required; all connection changes are achieved via the management console using the functions of the MMB. This not only speeds reallocation of resources, it avoids cabling errors, and frees up precious PCI slots for other uses.

The System Mirror, is the same super-reliability found in top-end mainframes. All addressing, data bus and memory operations are duplexed for total operational redundancy and maximum processor utilization.

Partitioning of resources, in particular, is very robust. Fujitsu has chosen a granular hardware partitioning technique that removes any potential for total system failure. Not only are partition faults isolated from adjoining partitions, but the removal of partition control software removes any potential for that to become a single point of failure.

PRIMEQUEST fast restart capability comes from the MMB's ability to pre-emptively detect faults. This enables the use of reserve system boards to configured and dynamically reallocated to problem partitions without a system halt.

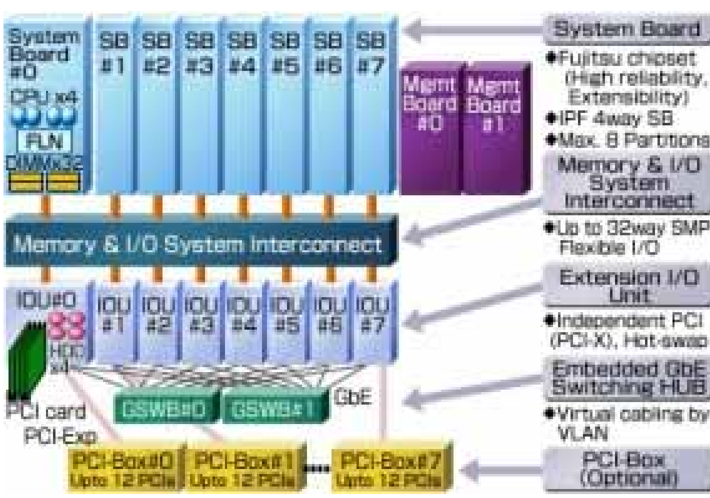

Finally structured design and flexible interconnects, ensure that only minimum resources are needed for each application. Systems can start small and grow as required. Processors, memory and I/O can be independently added using separate, flexibly configured, system boards, I/O Units and PCI boxes.

PRIMEQUEST reduces operational costs

PRIMEQUEST's flexibility makes it ideal for mixed workloads. Resource priority control enables the right processor resources to be set up for each task. Once minimum resource allocations are set any unused resources can be assigned to higher priority tasks as workloads and performance demands change. This reduces setup costs and enables more accurate and incremental addition of resources as demand grows.

For example, PRIMEQUEST is able to ensure that every application is a perfect fit to the available resources. Compare this with the use of Blade servers. No resources are wasted and no applications need be constrained by fixed resource boundaries. PRIMREQUEST's 'on-demand' environment fully maximises return on infrastructure investment across the lifetime of the system, balanced with the best possible response to users at all times.

PRIMEQUEST reduces the cost of physical infrastructure management by allowing up to 8 concurrent Linux and Windows system partitions to operate in the same highly available system 'frame'. The in-built systems management reduces administration overheads and the reduced footprint of a single system saves floor space, reduces power consumption and centralizes operational tasks.

System migration costs can also be reduced, as PRIMEQUEST supports side-by-side matched environments. Ideal for migrating 32 bit applications to 64 bit operation, or testing upgrades to operational systems; evaluation, validation and performance tuning is simpler. Importantly, final system switchover is easier and simpler as the infrastructure remains unchanged with only the I/O connections switched to the live database.

The flexible I/O capability of PRIMEQUEST removes the cost of expensive add-on I/O port devices. I/O is always "independent" of partitions. Reconfiguration or partition swaps can be performed without cable changes and operational system restarts are achieved in minutes rather than hours.

By following the Intel 64-bit processor roadmap and enabling multi-generation processor upgrades, PRIMEQUEST extends the life of the overall IT investment. This means on-going and lower cost performance growth within the same environment and an extend lifecycle for the refurbishment and investment maximization of major business applications.

Finally to ensure overall success of PRIMEQUEST, Fujitsu has entered into a large range of partnerships with organizations dedicated to development in the Linux and Windows space. This will ensure that PRIMEQUEST product development and innovation continues to match major developments and business trends as well as meet the requirements of users along the road to autonomous computing and beyond.

Major partners (in alphabetical order) include: BEA Systems, Inc., BMC Software, Inc., Computer Associates International, Inc., EMC Corporation, Intel Corporation, Microsoft Corporation, Network Appliance, Inc., Novell, Inc., Oracle Corporation, Red Hat, Inc., SAP AG, Softek Storage Solutions Corporation, VERITAS Software Corporation.

INDUSTRY NEWS

Cray Announcements:

Software Cradle (SC), a prominent Japanese CFD application developer, has chosen the Cray XD1 Opteron/Linux-based supercomputer as the company's platform for software development and consulting. SC's Cray XD1 installation consists of six chassis and 72 AMD Opteron processors.

CD-adapco, a CFD consulting and software firm, has purchased a six-chassis, 72-AMD Opteron processor Cray XD1 supercomputer to meet the increasing computational demands of a broad range of CFD problems.

Cray and LSTC announced it has certified LS-DYNA for operation on the Cray XD1 system.

MSC.Nastran 2005 r2

Major new features and enhancements are in the areas of nonlinear, optimization, and high performance computing and include:

- MSC.Nastran DMP Product Module Enhancements - new Multilevel DMP (Distributed Memory Parallel) capability has been added to increase solver performance with more highly scalable algorithms for high performance computing environments.
- MSC.Nastran Implicit Nonlinear Product Module - A set of major and minor enhancements have been made to greatly improve the performance and capabilities when accessing the nonlinear capabilities of MSC.Marc through existing MSC.Nastran models.
- MSC.Nastran Explicit Nonlinear Product Module (pre-release) - A new solution sequence (SOL 700) that allows engineers to access the capabilities of the MSC.Dytran LS-DYNA solver to perform crash and drop test analysis using their existing MSC.Nastran models.

ASIA PACIFIC NEWS

LS-DYNA Conferences

Korea 11/25/05 (THEME) **Korean LS-DYNA Users Conference**
Japan 11/29-30/05 (JRI) **Japanese LS-DYNA Users Conference (Nagoya)**

FEA Information is proud to display our first co-advertisement in China.

As published in the Summer 2005 Edition of Automotive Manufacturer

Available Paper(s) -
www.feapublications.com Menu Link: “Featured”

The following paper is now posted on line:

Transient Response of a Projectile in Gun Launch Simulation Using Lagrangian and ALE Methods

Ala Tabiei – Department of Aerospace Engineering & Engineering Mechanics, University of Cincinnati, OH 45221-0070

Mostafiz R. Chowdhury – U.S. Army Research Laboratory, 2800 Powder Mill Road, Adelphi, MD 20783-1145

ABSTRACT:

This paper describes the usefulness of Lagrangian and arbitrary Lagrangian/Eulerian (ALE) methods in simulating the gun launch dynamics of a generic artillery component subjected to launch simulation in an air gun test. Lagrangian and ALE methods are used to simulate the impact mitigation environment in which the kinetic energy of a projectile is absorbed by the crushing of an aluminum honeycomb mitigator. Issues related to the effectiveness of these methods in simulating a high degree of distortion of Aluminum honeycomb mitigator with the commonly used material models (metallic honeycomb and crushable foam) are discussed. Both computational methods lead to the same prediction for the deceleration of the test projectile and are able to simulate the behavior of the projectile. Good agreement between the test results and the predicted projectile response is achieved via the presented models and the methods employed.

RESUME:

Phillip H. Burnside, Ph.D.
H: (760) 956-2140
C: (760) 646-0764
Email: rmburnside@verizon.net
11340 Muscatel St.
Hesperia, CA 92345

Summary:

My engineering career has been focused on the application of numerical modeling and computational fluid analysis to solve a diverse set of engineering problems. These problems occurred in very complex production processes where small changes in one area would have a major impact on production output, and modeling these changes was the only economical method of evaluation. In solving these problems, I have frequently partnered with the various software companies to develop Code Revisions enabling problem solutions to previously unsolvable problems.

Work Experience

Sr. Process Engineer – James Hardie Building Products, Fontana, CA 2002 – 2005

The Process Engineering Group's mission is two fold: (1) apply new technology to existing processes and (2) take new processes and products from the R&D stage to commercialization. . My primary task is to generate new ideas and concepts to solve the challenges of getting a new process or product out into the field and to investigate ongoing field process problems occurring in mature processes. In order to obtain solutions to many of the challenging technical problems we faced has required pushing the envelope of these analytical tools. I have frequently worked with ALGOR, LS-DYNA and FLUENT to development Code Revisions adding new sets of physics so that we could solve difficult and complex problems.

In addition, I have solved many of the highly technical process and product challenges that contributed to an increase in the amount of product coming off of various Fiber Cement manufacturing lines. For example (1) I developed a modification to the Pipes manufacturing line that improved the uniformity of the dewater that occurs as the laminate structure of the pipe is laid up to form a pipe. I used the ALGOR FEA Code and the Fluent CFD code to define the root cause of the problem and model the solution. We then implemented this design modification to the process line. This resulted in a significant increase in the line speed and thereby the total through put of the manufacturing line for pipes. (2) I looked at how to improve uptime on the sheet product manufacturing line. To do this I focused in on the mixing tanks and curing ovens using the Fluent CFD code to validate my theories and to design a solution. When implemented, these concepts resulted in two to four percent increase in up time across several production lines. (3) I used ALGOR and LS-DYNA to assist in the design of a fiber-cement fencing product to compete with wood fencing. Initial experimental static testing implied that the fiber cement fence was significantly better. However; the fiber-cement fencing failed a test of an object hitting it at 80mph. I developed a set of models that were used to redefine the fencing design so that the fiber-cement fencing would pass the required impact field-test.

As a one of the corporation's highly technically skilled engineers, I served as the technical screener of engineers for the corporation. I have personally recruited many of the engineers in the Central Process Engineering group and also for the design and research engineering groups. I also provide technical training and project guidance for new hire engineers.

Sr. Associate Engineer – PPG Industries, Pittsburgh, PA 1997 – 2002

My primary assignment was to develop the use of both Finite Element Analysis (FEA) and Computational Fluid Dynamics (CFD) codes as tools in (1) the design phase of new OEM glass products and (2) the fabrication process design for making these products. This involves the use of parallel computing machines in order to get quick and comprehensive solutions for use by product designers. A combination of LS-DYNA, ANSYS and the ALGOR FEA codes were used for structural problems and the FLUENT CFD code was used for solving flow and heat transfer problems. This type of analysis was used to illustrate the feasibility of new designs for potential customers.

Research Assistant - MAE Department, West Virginia University, Morgantown, WV. 1991 – 1997

During this time period I attended WVU and worked on my Doctoral Dissertation involving research on how to perform a thermal stress analysis of a unique, new rotary engine design. In order to achieve this goal, a Fortran code on combustion, developed by NASA, was modified to take into account the unique characteristics of this rotary engine design. The ALGOR finite element code was used for thermal conduction and stress calculations and the CFX-5 CFD code, which was used to define the heat loss to the cooling system.

Also During this time I worked full time to support my family and held the following engineering positions:

Sales / Applications Engineer - AEA Technology, Pittsburgh, PA 1996 - 1997
As a Sales/Application engineer, I provided potential customers of the CFX family of CFD software with guidance on how the technology could be applied to their process.

Applications Engineer - Algor Inc., Pittsburgh, PA 1995 - 1996
My primary assignment was to provide technical support and training. As a part of these tasks, I developed a standardized set of training seminars on subjects ranging from an introduction dynamics for the ALGOR.

Consulting Engineer - Pittsburgh, PA 1994 - 1995
I worked for several companies in Western Pennsylvania on a contractual basis to solve a wide range of engineering prob-

lems. These challenges ranged from the design of support systems for precision reflecting mirrors, evaluation of robotic parts, to new concept bridge designs using both ANSYS and ALGOR FEA software codes.

Applications Engineer - Mallett Technology Inc., McMurray, PA. 1992 -1994
The primary assignment was providing engineering support for companies using the ANSYS FEA program. In the process of providing training and support on wide range of subjects for the ANSYS and Pro/E software codes, I was also a member of the engineering team providing consulting services that tested our engineering knowledge and creativity to solve design issues by using these codes as design tools.

Mechanical Engineer - Murray Corporation, Baltimore, MD. 1988 - 1991

Mechanical Engineer - Newport News Shipbuilding, Newport News, VA. 1987 – 1988

Accomplishments in the Naval Reserve

USS SAN FRANCISCO (2005): At the beginning of 2005, the USS SAN FRANCISCO experienced grave damage to the bow of the submarine when it ran into an uncharted underwater mountain at flank speed. I was the part of the repair team sent to Guam who preformed two major structural analyses of the boat. First, as a part of this effort, a complete structural model of the front of the boat was created to validate the design of the temporary bow that is being built. The temporary bow must withstand the rigors of surface ocean travel back to the states for final repair. Second, an impact model of the whole sub was created in LS-DYNA. This model will be used to determine if any areas away from the bow, that are not readily accessible, may also have potentially been damaged.

Navy Achievement Award – USS PORT ROYAL (2002-2003): During a structural assessment inspection of the USS PORT ROYAL, several structural members near the bottom of the hull in the engine room where found to be almost completely corroded away. This area was identified by the crew as the only section of hull that would flex in and out during heavy seas. A structural analysis of the area hull was preformed using the ALGOR finite element code. The results of this analysis illustrated that the hull in this area was in danger of failing due to low cycle fatigue. Since this is single hull ship, emergency welding to the hull was not option in the short term. A simple solution was identified where ships crew could use standard emergency shoring beams and bolt them next to the corroded beams in order to stabilize the hull until the ship would be put in dry-docking a year later for it's normal maintenance cycle.

Navy Commendation – USS COLE (2000-2001): During the repair of the USS COLE a 80,000 pound propeller shaft was dropped onto a deck structure while being rigged into the ship. During a visible inspection no damage was detected on the shaft. However: in order to do a NDT to verify that shaft was safe to use, the shaft would have to be installed on its bearings; and if bad, removal and replacement would cause a three month delay in the repair. Or if the shaft was removed and a new one put in, it would take three months to remove and replace it. Based on details available I preformed an impact analysis with ANSYS and LS-DYNA over a 48 hour period and was able to prove that it was safe to use the shaft. The analysis revealed that the equipment that was crushed absorbed the energy from the impact. The USS COLE went back into service on time and is now serving with distinction.

Engineering Duty Officer – 1445/LCDR
Active DOD Secret Clearance

Education

Ph.D. in Mechanical Engineering - West Virginia University May 1997
Dissertation *"A comparison of the Pin Cam and Inverted Pin Cam designs of the Axial Vane Rotary Engine"*
M.S. in Mechanical Engineering - West Virginia University May 1992
Thesis *"Design Optimization of Fiber-Reinforced Composite-Material Guide Way for MAGLEV"*
B.S. in Mechanical Engineering - West Virginia University May 1987

AFFILIATIONS/Notes:
American Society of Mechanical Engineers
United States Naval Reserve - Engineering Duty Officer Designator 1445 - LCDR
Naval Reserve Officers Association
Naval Reserve Association
List of Publications is available upon request

EVENTS

May 10, 2005
16th Annual HP Technology Trend in Automotive Engineering Symposium - Plymouth, MI

May 31 – June 03, 2005
Dresden, Germany
Third Joint ANSYS CFX & FZR Workshop on Multiphase Flows

May 17-20, 2005
LeMeridien, St. Julians, Malta
NAFEMS World Congress

May 25-26, 2005
5th European LS-DYNA Conference
The ICC, Birmingham UK (ARUP)

June 06-09, 2005
Westin Harbour Castle, Toronto, Ontario, Canada
AIAA Fluid Dynamics Conference & Exhibit

June 6-10, 2005
HP Software Forum, Denver, CO

June 13-17, 2005
Group (SGIUG) – Munich Germany

June 25-27, 2005
8th U.S. National Congress on Computational Mechanics, Austin, TX

October 05-08, 2005
TCN CAE 2005 International Conference on CAE and Computational Technologies for Industry
Italy – (Numerica)

October 20-21, 2005
German-LS-DYNA Forum
(DYNAmore)
Bamberg, Germany

November 09-11, 2005
23rd CADFEM Users' Meeting – Int'l Congress on FEM Tech. W/ANSYS CFX & ICEM CFD Conference, Bonn, Germany

November 25, 2005
Korean Users Conferece –
LS-DYNA (THEME)

November 29-30, 2005
Japanese Users Conference
(Nagoya) LS-DYNA (JRI)

June 2006
LS-DYNA
9th International LS-DYNA Users Conference – Deerborn, MI
(LSTC)

LS-DYNA Resource Page

Interface - Hardware - OS And General Information

LS-DYNA General Information- www.lstc.com sales@lstc.com

Version: 970

Classes:
www.lstc.com classes

30-day demonstration licenses available – no fee

Sales
sales@lstc.com

Participant Hardware and OS that run LS-DYNA (alpha order)

All Hardware and OS listed have been fully QA'd by Livermore Software Technology Corporation

AMD Opteron Linux	HP PA8000 HPUX	INTEL IA32 Linux, Windows	SGI Mips IRIX6.5
CRAY XD1 Linux	HPIA64 HPUX or Linux	INTEL IA64 Linux	SGI IA64 Altix
FUJITSU Prime Power SUN OS 5.8	HP Alpha True 64	INTEL Xeon EMT64 Linux	
FUJITSU VPP Unix System V	IBM Power 4/5 AIX 5.1	NEC SX6 Super-UX	

LS-DYNA Resource Page

Participant Software Interfacing or embedding LS-DYNA

Each software program can interface to all, or a very specific and limited segment of the other software program. The following list are software programs interfacing to or having the LS-DYNA solver embedded within their product. For complete information on the software products visit the corporate website.

ANSYS - ANSYS/LS-DYNA
www.ansys.com/products/environment.asp

ANSYS/LS-DYNA - Built upon the successful ANSYS interface, ANSYS/LS-DYNA is an integrated pre and postprocessor for the worlds most respected explicit dynamics solver, LS-DYNA. The combination makes it possible to solve combined explicit/implicit simulations in a very efficient manner, as well as perform extensive coupled simulations in Robust Design by using mature structural, thermal, electromagnetic and CFD technologies.

AI*Environment: A high end pre and post processor for LS-DYNA, AI*Environment is a powerful tool for advanced modeling of complex structures found in automotive, aerospace, electronic and medical fields. Solid, Shell, Beam, Fluid and Electromagnetic meshing and mesh editing tools are included under a single interface, making AI*Environement highly capable, yet easy to use for advanced modeling needs.

ETA – DYNAFORM
www.eta.com

Includes a complete CAD interface capable of importing, modeling and analyzing, any die design. Available for PC, LINUX and UNIX, DYNAFORM couples affordable software with today's high-end, low-cost hardware for a complete and affordable metal forming solution.

ETA – VPG
www.eta.com

Streamlined CAE software package provides an event-based simulation solution of nonlinear, dynamic problems. eta/VPG's single software package overcomes the limitations of existing CAE analysis methods. It is designed to analyze the behavior of mechanical and structural systems as simple as linkages, and as complex as full vehicles

MSC.Software
“MSC.Dytran LS-DYNA”
www.msc.software.com

Tightly-integrated solution that combines MSC.Dytran's advanced fluid-structure interaction capabilities with LS-DYNA's high-performance structural DMP within a common simulation environment. Innovative explicit nonlinear technology enables extreme, short-duration dynamic events to be simulated for a variety of industrial and commercial applications on UNIX, Linux, and Windows platforms. Joint solution can also be used in conjunction with a full suite of Virtual Product Development tools via a flexible, cost-effective MSC.MasterKey License System.

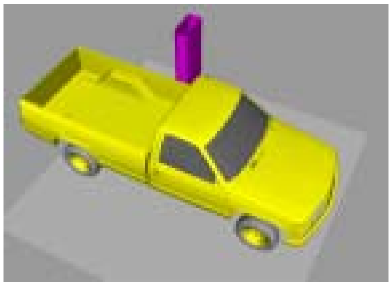

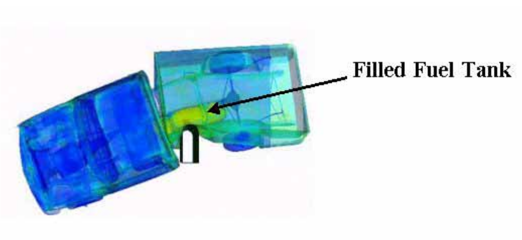

Side Impact With Fuel Oil Inside

MSC.Software - MSC.Nastran/SOL 700

The MSC.Nastran™ Explicit Nonlinear product module (SOL 700) provides MSC.Nastran users the ability access the explicit nonlinear structural simulation capabilities of the MSC.Dytran LS-DYNA solver using the MSC.Nastran Bulk Data input format. This product module offers unprecedented capabilities to analyze a variety of problems involving short duration, highly dynamic events with severe geometric and material nonlinearities.

MSC.Nastran Explicit Nonlinear will allow users to work within one common modeling environment using the same Bulk Data interface. NVH, linear, and nonlinear models can be used for explicit applications such as crash, crush, and drop test simulations. This reduces the time required to build additional models for another analysis programs, lowers risk due to information transfer or translation issues, and eliminates the need for additional software training.
The MSC.Nastran Sol 700 will be released in November 2005. Beta release is available now !

MSC.Software – Gateway for LS-DYNA

Gateway for LS-DYNA provides you with the ability to access basic LS-DYNA simulation capabilities in a fully integrated and generative way. Accessed via a specific Crash workbench on the GPS workspace, the application enhances CATIA V5 to allow finite element analysis models to be output to LS-DYNA and then results to be displayed back in CATIA. Gateway for LS-DYNA supports explicit nonlinear analysis such as crash, drop test, and rigid wall analysis.

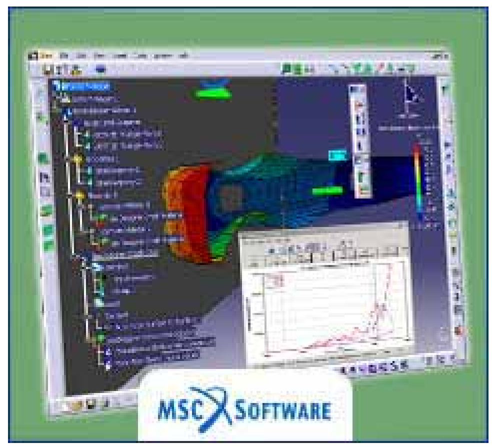

Gateway products provide CATIA V5 users with the ability to directly interface with their existing corporate simulation resources, and exchange and archive associated simulation data.

Oasys software for LS-DYNA
www.arup.com/dyna

Oasys software is custom-written for 100% compatibility with LS-DYNA. Oasys PRIMER offers model creation, editing and error removal, together with many specialist functions for rapid generation of error-free models. Oasys also offer post-processing software for in-depth analysis of results and automatic report generation.

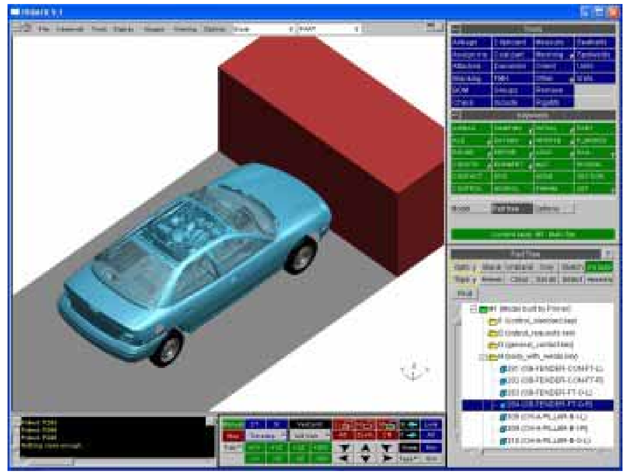

LS-DYNA Events

UK 05/25-26/05 (Arup) **5th European LS-DYNA Conference**
Italy 10/05-10/06 (Numerica) **(Numerica)** **TCN CAE 2005 International Conference on CAE and Computational Technologies for Industry -** workshops focusing on LS-DYNA
Germany - 10/20-10/21 (DYNAmore) **German LS-DYNA Forum**
Germany - 11/09-11/11 (CADFEM) **Int'l Congress on FEM Tech.. workshops focusing on LS-DYNA**
Korea 11/25/05 (THEME) **Korean LS-DYNA Users Conference**
Japan 11/29-30/05 (JRI) **Japanese LS-DYNA Users Conference (Nagoya)**
US 06/06 (LSTC) **9th International LS-DYNA Users Conference**

Hardware & Computing and Communication Products

www.amd.com

www.fujitsu.com

www.hp.com

www-1.ibm.com/servers/deepcomputing

www.intel.com

www.nec.com

www.sgi.com

www.cray.com

Software Distributors

Alphabetical order by Country

Australia	**Leading Engineering Analysis Providers** www.leapaust.com.au
Canada	**Metal Forming Analysis Corporation** www.mfac.com
China	**ANSYS China** www.ansys.cn
China	**MSC. Software – China** www.mscsoftware.com.cn
Germany	**CAD-FEM** www.cadfem.de
Germany	**Dyna*More*** www.dynamore.de
India	**GissETA** www.gisseta.com
India	**Altair Engineering India** www.altair.com
Italy	**Altair Engineering Italy** www.altairtorino.it
Italy	**Numerica SRL** www.numerica-srl.it
Japan	**Fujitsu Limited** www.fujitsu.com
Japan	**The Japan Research Institute** www.jri.co.jp
Japan	**CRC Solutions Corp.** www.engineering-eye.com
Korea	**Korean Simulation Technologies** www.kostech.co.kr
Korea	**Theme Engineering** www.lsdyna.co.kr

Software Distributors (cont.)

Alphabetical order by Country

Netherlands	**Infinite Simulation Systems B.V** www.infinite.nl
Russia	**Strela, LLC** www.ls-dynarussia.com
Sweden	**Engineering Research AB** www.erab.se
Taiwan	**Flotrend** www.flotrend.com.tw
Turkey	**FIGES** www.figes.com.tr
USA	**Altair Western Region** www.altair.com
USA	**Engineering Technology Associates** www.eta.com
USA	**Dynamax** www.dynamax-inc.com
USA	**Livermore Software Technology Corp.** www.lstc.com
USA	**ANSYS Inc.** www.ansys.com
UK	**Oasys, LTD** www.arup.com/dyna/

Consulting and Engineering Services

Alphabetical Order By Country

Australia Manly, NSW www.leapaust.com.au	**Leading Engineering Analysis Providers** Greg Horner info@leapaust.com.au 02 8966 7888
Canada Kingston, Ontario www.mfac.com	**Metal Forming Analysis Corporation** Chris Galbraith galb@mfac.com (613) 547-5395
India Bangalore www.altair.com	**Altair Engineering India** Nelson Dias info-in@altair.com 91 (0)80 2658-8540
Italy Torino www.altairtorino.it	**Altair Engineering Italy** sales@altairtorino.it
Italy Firenze www.numerica-srl.it	**Numerica SRL** info@numerica-srl.it 39 055 432010
UK Solihull, West Midlands www.arup.com	**ARUP** Brian Walker brian.walker@arup.com 44 (0) 121 213 3317
USA Irvine, CA www.altair.com	**Altair Engineering Inc. Western Region** Harold Thomas info-ca@altair.com
USA Windsor, CA www.schwer.net/SECS	**SE&CS** Len Schwer len@schwer.net (707) 837-0559

Educational & Contributing Participants

Alphabetical Order By Country

China	Dr. Quing Zhou	Tsinghua University
India	Dr. Anindya Deb	Indian Institute of Science
Italy	Professor Gennaro Monacelli	Prode – Elasis & Univ. of Napoli, Frederico II
Russia	Dr. Alexey I. Borovkov	St. Petersburg State Tech. University
USA	Dr. Ted Belytschko	Northwestern University
USA	Dr. David Benson	University of California – San Diego
USA	Dr. Bhavin V. Mehta	Ohio University
USA	Dr. Taylan Altan	The Ohio State U – ERC/NSM
USA	Dr. Ala Tabiei	University of Cincinnati
USA	Tony Taylor	Irvin Aerospace Inc.

Informational Websites

FEA Informationwebsites	www.feainformation.com
TopCrunch – Benchmarks	www.topcrunch.org
LS-DYNA Examples (more than 100 Examples)	www.dynaexamples.com
LS-DYNA Conference Site	www.ls-dynaconferences.com
LS-DYNA Publications to Download On Line	www.dynalook.com
LS-DYNA Publications	www.feapublications.com
LS-DYNA Forum	http://portal.ecadfem.com/Forum.1372.0.html
LS-DYNA CADFEM Portal	http://www.lsdyna-portal.com

Archived News Page

March 07

- Infinite Simulations Systems, B.V.e - New Participant –
- New AVI #610
- FUJITSU Primepower 2500
- AMD Opteron processors
- Dynamax – Distributor US

March 14

- NEC Itanium 2 Blade Server
- IBM Deep Computing
- ERAB –Distributor Sweden
- THEME – Distributor Korea

March 21

- CRAY XD! Overview
- ANSYS DesignXplorer VT
- CRC Distributor Japan
- Altair Western Region Distributor US

Top Crunch News

Dr. David Benson
www.topcrunch.org

Yong-Cheng Liu at ANSYS, Inc. has provided Top Crunch with a parallel implicit benchmark problem.

The problem has been run up to 32 processors.

This benchmark will complement the parallel explicit benchmark problems from LSTC.

The input file, along with the instructions on running it, are available on the downloads page of Top Crunch.

Computational Plasticity Part II: Integration of the Plasticity Equations

David J. Benson
Dept. of Mechanical and Aerospace Engineering
University of California, San Diego
dbenson@ucsd.edu

1 Radial Return

The most popular method for integrating the plasticity equations for isotropic von Mises plasticity is *radial return*, developed by Wilkins for HEMP and Maenchen and Sack for TENSOR, two finite difference codes developed at Lawrence Livermore National Laboratory. It has been generalized to arbitrary convex yield surfaces and yield stress functions, although the "return" portion of the algorithm is no longer radial. Conceptually, the idea is quite simple: first the stress is updated assuming that the response is elastic, then if it is outside the yield surface, the stress is projected on to the closest point of the yield surface (Figure 1). If the material is perfectly plastic, the yield surface is constant, but if $h > 0$, the yield surface expands during the plastic flow, and the stress is projected on the expanded yield surface. The data available at the beginning of the radial return update is the previous stress, equivalent plastic strain, and increment in the strain across the time step, $\triangle\boldsymbol{\epsilon} = \triangle t\dot{\boldsymbol{\epsilon}}$. By the end of the radial return procedure, the stress and equivalent plastic strain have been updated. The superscripts n and $n+1$ are dropped to simplify the notation in this section, and to make the equations in this section look as close to their actual appearance within a computer code as possible, where the old values are overwritten by the new values.

The *trial stress*, $\boldsymbol{\sigma}^{Tr}$, is the deviatoric part of the stress calculated assuming that the response is elastic,

$$\boldsymbol{\sigma}^{Tr} = \boldsymbol{\sigma}' + 2\mu\triangle\boldsymbol{\epsilon}' \tag{1}$$

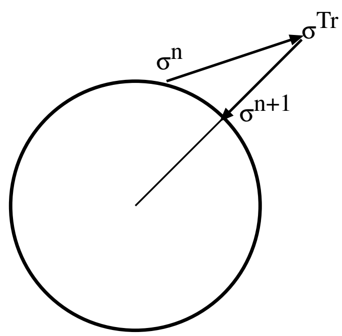

Figure 1: Schematic of radial return.

but since the pressure is independent of the plastic flow, its update is the same regardless of whether or not there is plastic flow,

$$P = P - (\lambda + \frac{2}{3}\mu)\mathrm{tr}(\triangle\boldsymbol{\epsilon}). \tag{2}$$

The equivalent trial stress is evaluated,

$$\bar{\sigma}^{Tr} = \sqrt{\frac{3}{2}\boldsymbol{\sigma}^{Tr} : \boldsymbol{\sigma}^{Tr}} \tag{3}$$

and if

$$\bar{\sigma}^{Tr} \leq \sigma_y = \sigma_y^0 + h\bar{\epsilon}^p \tag{4}$$

then the response is elastic, and the stress at the end of the time step is

$$\boldsymbol{\sigma} = \boldsymbol{\sigma}^{Tr} - P\boldsymbol{I}. \tag{5}$$

When Equation 4 isn't satisfied, there is plastic flow, and the increment in the equivalent plastic strain must be calculated. The closest point of the yield surface to the trial stress lies along the line from the origin to the trial stress, and therefore the final deviatoric stress will be proportional to the trial stress, $\boldsymbol{\sigma'} = \alpha\boldsymbol{\sigma}^{Tr}$. Regardless of the proportionality constant, the normal direction is

$$\boldsymbol{n} = \frac{\sqrt{3/2}}{\bar{\sigma}^{Tr}}\boldsymbol{\sigma}^{Tr}. \tag{6}$$

The increment in equivalent plastic strain is calculated by requiring that the final equivalent stress equals the final yield stress,

$$\sqrt{\frac{3}{2}\boldsymbol{\sigma'} : \boldsymbol{\sigma'}} = \sigma_y^n + h\triangle\bar{\epsilon}^p \tag{7}$$

where $\sigma_y^n = h\bar{\epsilon}^p$ and

$$\begin{aligned}
\boldsymbol{\sigma}' &= \boldsymbol{\sigma}^{Tr} - 2\mu\boldsymbol{\epsilon}' && (8)\\
&= \boldsymbol{\sigma}^{Tr} - 2\mu\Lambda\boldsymbol{n} && (9)\\
&= \boldsymbol{\sigma}^{Tr} - 2\mu\left(\sqrt{3/2}\triangle\bar{\epsilon}^p\right)\left(\frac{\sqrt{3/2}}{\bar{\sigma}^{Tr}}\boldsymbol{\sigma}^{Tr}\right) && (10)\\
&= \left(1 - \frac{3\mu\triangle\bar{\epsilon}^p}{\bar{\sigma}^{Tr}}\right)\boldsymbol{\sigma}^{Tr} && (11)
\end{aligned}$$

Substituting in the last equation into Equation 7 results in a linear equation for the increment in equivalent plastic strain,

$$\left(1 - \frac{3\mu\triangle\bar{\epsilon}^p}{\bar{\sigma}^{Tr}}\right)\bar{\sigma}^{Tr} = \sigma_y^n + h\triangle\bar{\epsilon}^p \quad (12)$$

so that, finally,

$$\triangle\bar{\epsilon}^p = \frac{\bar{\sigma}^{Tr} - \sigma_y^n}{3\mu + h}. \quad (13)$$

Once the increment in equivalent plastic strain is calculated, the proportionality factor is calculated and the trial stress is scaled back to the yield surface. The stress update is completed by adding the deviatoric and mean stress, $-P$.

$$\begin{aligned}
\alpha &= \left(1 - \frac{3\mu\triangle\bar{\epsilon}^p}{\bar{\sigma}^{Tr}}\right) && (14)\\
\boldsymbol{\sigma}' &= \alpha\boldsymbol{\sigma}^{Tr} && (15)\\
\boldsymbol{\sigma} &= \boldsymbol{\sigma}' - P\boldsymbol{I} && (16)\\
\bar{\epsilon}^p &= \bar{\epsilon}^p + \triangle\bar{\epsilon}^p && (17)
\end{aligned}$$

2 Generalizing the Yield Function

The linear yield function given by $\sigma_y = \sigma_y^0 + h\bar{\epsilon}^p$ is too simple for many applications. A more general, nonlinear form, $\sigma_y(\bar{\epsilon}^p, \dot{\bar{\epsilon}}^p, \ldots)$ is easily incorporated within the radial return framework. The only two places where the yield function appears in the previous derivation are in determining if plastic flow occurs, Equation 4, and the discrete consistency condition for determining the increment in plastic strain, Equation 7.

Equation 4 generalizes to

$$\bar{\sigma}^{Tr} \leq \sigma_y(\bar{\epsilon}^p, 0, \ldots). \tag{18}$$

where the plastic strain rate is assumed to be zero to be consistent with the assumption that the update is elastic.

In a similar manner, Equation 4 generalizes to

$$\bar{\sigma}^{Tr} - 3\mu\triangle\bar{\epsilon}^p = \sigma_y(\bar{\epsilon}^p + \triangle\bar{\epsilon}^p, \triangle\bar{\epsilon}^p/\triangle t, \ldots), \tag{19}$$

giving a nonlinear equation that may be solved iteratively. From continuum mechanics, we know that the increment in plastic strain lies somewhere between zero and the entire strain increment, $\triangle\boldsymbol{\epsilon}$. The increment in equivalent plastic strain, therefore, must lie somewhere between 0 and $\sqrt{(2/3)\triangle\boldsymbol{\epsilon}' : \triangle\boldsymbol{\epsilon}'}$, and the equation may be solved with an iterative method that is guaranteed to converge (eventually).

The yield stress of many materials is a function of the temperature, T, with the yield strength decreasing as the temperature increases. Heat transfer, and the work associated with the stress, alter the temperature. Most finite element analyses that couple heat transfer with the mechanical solution do so loosely, that is, the geometry is held fixed during the heat conduction and there is no heat conduction during the mechanical equilibrium solution. Discussing the coupling algorithms is beyond the scope of the present discussion, but extending Equation 19 to include the effects of temperature through the plastic work is not difficult.

From the energy equation, the temperature evolves (to second order accuracy) according to

$$T^{n+1} = T^n + \frac{1}{2C}\left(\boldsymbol{\sigma}^n + \boldsymbol{\sigma}^{n+1}\right)\triangle\boldsymbol{\epsilon} \tag{20}$$

where C is the heat capacity. Assuming that the step is plastic, the temperature evolution may be approximated to first order accuracy as

$$T^{n+1} = T^n + \frac{1}{C}\sigma_y\triangle\bar{\epsilon}^p. \tag{21}$$

Equation 19 becomes

$$\bar{\sigma}^{Tr} - 3\mu\triangle\bar{\epsilon}^p = \sigma_y(\bar{\epsilon}^p + \triangle\bar{\epsilon}^p, \triangle\bar{\epsilon}^p/\triangle t, T^{n+1}, \ldots) \tag{22}$$

where T^{n+1} is updated using the values from the previous iteration.

When thermal softening occurs, the increment in plastic strain can exceed the total strain increment. Iterative methods that require a bounding interval for the solution may fail in this situation if the upper bound on the equivalent plastic strain is based on the total strain increment. Since the final yield stress is greater than, or equal to, zero, the increment on equivalent plastic strain is bounded by

$$\triangle\bar{\epsilon}^p_{\max} = \sqrt{\frac{2}{3}\frac{\boldsymbol{\sigma}^{Tr}}{\mu} : \frac{\boldsymbol{\sigma}^{Tr}}{\mu}} = \frac{2}{3\mu}\bar{\sigma}(\boldsymbol{\sigma}^{Tr}). \tag{23}$$

3 The Consistent Tangent Matrix

In the evaluation of the tangent stiffness matrix, the material tangent matrix is required. The continuum tangent matrix was developed in a previous article, and it is frequently used in finite element calculations. A slightly different tangent matrix, however, is derived by differentiating the radial return stress update with respect to the increment in the strain. The finite element literature refers to the latter matrix as the *consistent tangent matrix* because it is consistent with the radial return algorithm. The difference between the two tangent matrices only appears in the terms associated with the deviatoric stress since the mean stress is updated elastically with radial return. Calculations performed with full Newton iteration exhibit quadratic convergence more frequently with the consistent tangent than the continuum tangent. However, finite element iterations only converge quadratically near the solution. When large load increments are applied, most of the iterations will converge at a linear rate at best regardless of the tangent. The benefit with a quasi-Newton method is less clear.

For clarity and to make its implementation more straight forward, the derivation is presented using index notation, and $\bar{\sigma}(\boldsymbol{\sigma}^{Tr})$ is simplified to $\bar{\sigma}$. Since the mean stress term is elastic, and, therefore its tangent is simply the associated elastic terms, only the deviatoric stress is considered.

$$\sigma'_{ij} = \left(1 - \frac{3\mu}{3\mu + h}\frac{\bar{\sigma} - \sigma_y}{\bar{\sigma}}\right)\sigma^{Tr}_{ij} \tag{24}$$

$$= \left(\frac{h}{3\mu + h} + \frac{3\mu}{3\mu + h}\frac{\sigma_y}{\bar{\sigma}}\right)\sigma^{Tr}_{ij} \tag{25}$$

The tangent matrix is evaluated by using the chain rule of differentiation,

$$\frac{\partial \sigma'_{ij}}{\partial \triangle \epsilon_{kl}} = \frac{\partial \sigma'_{ij}}{\partial \triangle \epsilon'_{mn}} \cdot \frac{\partial \triangle \epsilon'_{mn}}{\partial \triangle \epsilon_{kl}}. \tag{26}$$

Evaluating the first derivative on the right hand side,

$$\begin{aligned}
\frac{\partial \sigma'_{ij}}{\partial \triangle \epsilon'_{mn}} &= \left(\frac{h}{3\mu + h} + \frac{3\mu}{3\mu + h}\frac{\sigma_y}{\bar{\sigma}}\right)\frac{\partial \sigma^{Tr}_{ij}}{\partial \triangle \epsilon'_{mn}} \\
&+ \frac{3\mu}{3\mu + h}\sigma_y \left[-\frac{1}{2} \cdot \frac{1}{\bar{\sigma}^3} \cdot \frac{3}{2} \cdot 2\sigma^{Tr}_{kl} \frac{\partial \sigma^{Tr}_{kl}}{\partial \triangle \epsilon'_{mn}}\right] \sigma^{Tr}_{ij} \qquad (27) \\
&= \left(\frac{h}{3\mu + h} + \frac{3\mu}{3\mu + h}\frac{\sigma_y}{\bar{\sigma}}\right)\frac{\partial \sigma^{Tr}_{ij}}{\partial \triangle \epsilon'_{mn}} \\
&- \left(\frac{3\mu}{3\mu + h}\right)\left(\frac{\sigma_y}{\bar{\sigma}}\right)\frac{\partial \sigma^{Tr}_{kl}}{\partial \triangle \epsilon'_{mn}} n_{ij} n_{kl} \qquad (28)
\end{aligned}$$

where

$$\frac{\partial \sigma^{Tr}_{ij}}{\partial \triangle \epsilon'_{mn}} = 2\mu \delta_{im} \delta_{jn}. \tag{29}$$

Substituting Equation 29 into Equation 28 gives

$$\begin{aligned}
\frac{\partial \sigma'_{ij}}{\partial \triangle \epsilon'_{mn}} &= 2\mu \left(\frac{h}{3\mu + h} + \frac{3\mu}{3\mu + h}\frac{\sigma_y}{\bar{\sigma}}\right) \delta_{mi} \delta_{nj} \\
&- 2\mu \left(\frac{3\mu}{3\mu + h}\right)\left(\frac{\sigma_y}{\bar{\sigma}}\right) n_{ij} n_{mn}. \qquad (30)
\end{aligned}$$

The deviatoric strain increment is

$$\triangle \epsilon'_{mn} = \triangle \epsilon_{mn} - \frac{1}{3}\delta_{mn} \triangle \epsilon_{jj} \tag{31}$$

and, therefore, the second term in Equation 26 is

$$\frac{\partial \triangle \epsilon'_{mn}}{\partial \triangle \epsilon_{kl}} = \delta_{mk} \delta_{nl} - \frac{1}{3}\delta_{kl} \delta_{mn}. \tag{32}$$

Adding the term for the mean strain, substituting Equation 32 into Equation 30, and simplifying, gives the final result,

$$
\begin{aligned}
\frac{\partial \sigma_{ij}}{\partial \triangle \epsilon_{kl}} &= (\lambda + \frac{2}{3}\mu)\delta_{ij}\delta_{kl} \\
&+ 2\mu\left(\frac{h}{3\mu + h} + \frac{3\mu}{3\mu + h}\frac{\sigma_y}{\bar{\sigma}}\right)\left(\delta_{ik}\delta_{jl} - \frac{1}{3}\delta_{kl}\delta_{ij}\right) \\
&- 2\mu\left(\frac{3\mu}{3\mu + h}\right)\left(\frac{\sigma_y}{\bar{\sigma}}\right)n_{ij}n_{kl}. \qquad (33)
\end{aligned}
$$

This tangent is only used when there is plastic flow, otherwise the elastic tangent is used. Note that as the strain increment approaches zero, the ratio $\sigma_y/\bar{\sigma}$ approaches unity, and therefore the first two terms on the right hand side become the standard tangent for linear, isotropic elasticity, and the consistent tangent becomes equal to the continuum tangent.

Some numerical difficulties, associated with the ill-conditioning of the consistent tangent, can occur when simultaneously the hardening, h, approaches zero, and the strain increment becomes large, making the ratio $\sigma_y/\bar{\sigma}$ small. Letting h go to zero, the tangent becomes

$$
\begin{aligned}
\frac{\partial \sigma_{ij}}{\partial \triangle \epsilon_{kl}} &= (\lambda + \frac{2}{3}\mu)\delta_{ij}\delta_{kl} \\
&- 2\mu\left(\frac{\sigma_y}{\bar{\sigma}}\right)\left(\delta_{ik}\delta_{jl} - \frac{1}{3}\delta_{kl}\delta_{ij} + n_{ij}n_{kl}\right) \qquad (34)
\end{aligned}
$$

and letting $\sigma_y/\bar{\sigma}$ approach zero then gives

$$
\frac{\partial \sigma_{ij}}{\partial \triangle \epsilon_{kl}} = (\lambda + \frac{2}{3}\mu)\delta_{ij}\delta_{kl} \qquad (35)
$$

which is simply the term associated with the pressure, i.e., all the terms associated with plasticity have gone to zero.

4 Solving Problems with Path Dependent Materials

Most nonlinear material models, like the plasticity model, are described by ordinary differential equations,

$$
\begin{aligned}
\dot{\boldsymbol{\sigma}} &= \boldsymbol{\Sigma}\left(\boldsymbol{\sigma}, \boldsymbol{h}, \dot{\boldsymbol{h}}, \dot{\boldsymbol{\epsilon}},\right) \qquad (36) \\
\dot{\boldsymbol{h}} &= \boldsymbol{H}\left(\boldsymbol{\sigma}, \boldsymbol{h}, \dot{\boldsymbol{\epsilon}}\right) \qquad (37)
\end{aligned}
$$

where $\boldsymbol{\Sigma}$ and $\boldsymbol{H}$ are the differential equations, $\boldsymbol{h}$ is a vector of history variables (e.g., equivalent plastic strain), and $\dot{\boldsymbol{\epsilon}}$ is the appropriate strain rate. The differential equations are shown as depending on the strain rate, and not the strain, to emphasize the dependence of the stress rate through the unknown velocity, $\dot{\boldsymbol{\epsilon}} = \boldsymbol{B}\boldsymbol{v}$. These equations are integrated forward in time at each Gauss point in each element using radial return.

$$\boldsymbol{\sigma}^{n+1} = \boldsymbol{\Sigma}_I\left(\boldsymbol{\sigma}^n, \boldsymbol{h}^n, \triangle\boldsymbol{\epsilon}, \triangle t\right) \quad (38)$$

$$\boldsymbol{h}^{n+1} = \boldsymbol{H}_I\left(\boldsymbol{\sigma}^n, \boldsymbol{h}^n, \triangle\boldsymbol{\epsilon}, \triangle t\right) \quad (39)$$

In these equations, $\boldsymbol{\Sigma}_I$ and $\boldsymbol{H}_I$ are the numerical integration methods for advancing the solution over the time increment $\triangle t$. The strain increment across the step is

$$\triangle\boldsymbol{\epsilon} = \boldsymbol{B}\triangle\boldsymbol{u} = \boldsymbol{B}\left(\boldsymbol{u}^{n+1} - \boldsymbol{u}^n\right) \quad (40)$$

and similarly,

$$\triangle\boldsymbol{h} = \boldsymbol{h}^{n+1} - \boldsymbol{h}^n. \quad (41)$$

In all the discussions about solving nonlinear equations, the current value of a function is calculated using the current value of the solution variables, i.e, $f_i = f(u_i)$ and $\boldsymbol{f}_i = \boldsymbol{u}(\boldsymbol{u}_i)$. The path dependence of the material response through its differential equations introduces a small but important point about how the residual vector should be actually evaluated. A simple model problem limited to small strains illustrates the issues.

Assume that for a one dimensional problem, the differential equation for the stress is

$$\dot{\sigma} = E\dot{\epsilon} - \sigma\dot{\epsilon}. \quad (42)$$

The first term on the right hand side is linear elasticity, expressed in a rate form, and the second term is similar to the one that arises in the Truesdell stress rate. Using forward Euler integration, the stress is updated with

$$\sigma^{n+1} = \sigma^n + E\triangle\epsilon - \sigma^n\triangle\epsilon \quad (43)$$

The increment in displacement across the step at iteration i, $\triangle\boldsymbol{u}_i$, is the sum of the i contributions from the previous iterations, $\delta\boldsymbol{u}_k$,

$$\triangle\boldsymbol{u}_i = \sum_{j=1}^{i}\delta\boldsymbol{u}_j. \quad (44)$$

The strain increment across the time step for iteration i is

$$\triangle\epsilon_i = \boldsymbol{B}\triangle\boldsymbol{u}_i = \boldsymbol{B}\left(\boldsymbol{u}_i^{n+1} - \boldsymbol{u}^n\right) \tag{45}$$

and, therefore, the strain increment is the sum of the individual increments for each iteration,

$$\triangle\epsilon_i = \boldsymbol{B}\sum_{j=1}^{i}\delta\boldsymbol{u}_j = \sum_{j=1}^{i}\boldsymbol{B}\delta\boldsymbol{u}_j = \sum_{j=1}^{i}\delta\epsilon_i. \tag{46}$$

A niave implementation of an iterative nonlinear solver would update the stress each iteration with

$$\sigma_{i+1}^{n+1} = \sigma_i^{n+1} + E\delta\epsilon_i - \sigma_i^{n+1}\delta\epsilon_i. \tag{47}$$

Suppose that the iterative solver converges in two iterations, giving the strain increment

$$\triangle\epsilon = \delta\epsilon_1 + \delta\epsilon_2 \tag{48}$$

or, alternatively,

$$\delta\epsilon_1 = \alpha\triangle\epsilon \quad \delta\epsilon_2 = (1-\alpha)\triangle\epsilon. \tag{49}$$

Starting with an initial stress σ_0 (and dropping the superscript for the time step), the stress after the first iteration is

$$\begin{aligned} \sigma_1 &= \sigma_0 + \alpha E\triangle\epsilon - \sigma_0\delta\epsilon_1 && (50)\\ &= \sigma_0 + (E-\sigma_0)\alpha\triangle\epsilon. && (51) \end{aligned}$$

The final stress is then

$$\begin{aligned} \sigma_2 &= \sigma_1 + (E-\sigma_1)\delta\epsilon_2 && (52)\\ &= \sigma_0 + (E-\sigma_0)\alpha\triangle\epsilon && (53)\\ &\quad + (E - \{\sigma_0 + (E-\sigma_0)\alpha\triangle\epsilon\})(1-\alpha)\triangle\epsilon && (54)\\ &= \sigma_0 + \alpha(1-\alpha)(E-\sigma_0)(\triangle\epsilon)^2 && (55) \end{aligned}$$

The final stress clearly depends on how the strain increment is partitioned between the two iterations, and achieves a maximum at $\alpha = 1/2$. Small changes in the iteration strategy can therefore alter the final stress even if the final displacement solution remains the same.

The stress update is made independent of the iterations by always updating the stress with the *current strain increment* and *the stress and history vector from the previous step*. In this example, σ_1 remains unchanged from Equation 50, while the final stress becomes

$$\sigma_2 = \sigma_0 + (E - \sigma_0)\triangle\epsilon. \tag{56}$$

More generally, using the notation in Equations 38 and 39, the correct stress and history vector updates within a nonlinear equation solver are

$$\boldsymbol{\sigma}_{i+1}^{n+1} = \boldsymbol{\Sigma}_I\left(\boldsymbol{\sigma}^n, \boldsymbol{h}^n, \triangle\boldsymbol{\epsilon}_i, \triangle t\right) \tag{57}$$

$$\boldsymbol{h}_{i+1}^{n+1} = \boldsymbol{H}_I\left(\boldsymbol{\sigma}^n, \boldsymbol{h}^n, \triangle\boldsymbol{\epsilon}_i, \triangle t\right). \tag{58}$$

Note that during the iteration, the solution at n and $n+1$ are referenced. Keeping a complete solution state, 1 through $n+1$, for every step requires a prohibitive amount of memory, so that only the last two states are kept: the last converged state, n, and the state that is being iterated on, $n+1$. After the iterative solution converges, the solution from $n+1$ is copied to the storage previously used for state n, the displacement increment over the step, $\triangle\boldsymbol{u}$, is set to zero, and time is advanced $t = t + \triangle t$. The overall solution algorithm is now ready to solve for the solution at $n+2$.